Inhibition of furin by serpin Spn4A from *Drosophila melanogaster*

Mareke Oley, Matthias C. Letzel, Hermann Ragg*

Department of Biotechnology, Faculty of Technology, University of Bielefeld, D-33501 Bielefeld, Germany

Received 20 July 2004; revised 20 September 2004; accepted 1 October 2004

Available online 13 October 2004

Edited by Judit Ovádi

Abstract The serpin gene *Spn4* from *Drosophila melanogaster* encodes multiple isoforms with alternative reactive site loops (RSL). Here, we show that isoform Spn4A inhibits human furin with an apparent k_{assoc} of 5.5×10^6 M^{-1} s^{-1}. The serpin forms SDS-stable complexes with the enzyme and the RSL of Spn4A is cleaved C-terminally to the sequence –Arg–Arg–Lys–Arg↓ in accord with the recognition/cleavage site of furin. Immunofluorescence studies show that Spn4A is localized in the endoplasmic reticulum (ER), suggesting that the inhibitor is an interesting tool for investigating the cellular mechanisms regulating furin and for the design of agents controlling prohormone convertases.

Keywords: Serpin; Furin; Protease inhibitor; Endoplasmic reticulum; *Drosophila melanogaster*

1. Introduction

Proteolytic events play a central role in development, innate immune response and other important aspects in the life cycle of *Drosophila* [1,2]. These proteolytic processes must be stringently regulated in order to maintain homeostasis. Part of this task is fulfilled by a class of protease inhibitors – the serpins – most of which act as suicide inhibitors that present their reactive site loop (RSL) to the catalytic cleft of target enzymes [3].

The *Drosophila melanogaster* genome encodes about 30 serpin genes [4], including *Spn4* (synonym: *Sp*4) [5]. At least ten different transcripts can be generated from this gene that may encode up to eight inhibitor variants [6]. Among these, isoform Spn4A attracted special attention due to specific sequence features. First, the presence of a putative N-terminal signal peptide in combination with a C-terminal –His–Asp–Glu–Leu (HDEL) sequence that may function as endoplasmic reticulum (ER) retrieval signal suggests that the protein can cycle between the ER and the secretory routes of the cell. Second, the RSL of Spn4A is dominated by a sequence of basic amino acids preceding the putative scissile bond that resembles the recognition/cleavage site of furin [7,8], a subtilase-like enzyme that plays an eminent role in the activation of pathogens and in the processing of many cellular and secreted proteins and peptides [9,10]. Mature mammalian furin localizes predominantly to post-ER compartments and can cycle between the trans-Golgi network and the cell surface [11,12]. The involvement of furin and related proteinases in many important events and diseases has evoked vivid interest in the development of inhibitors and the processes regulating these enzymes. The recently published crystal structure of catalytic and P-domain of mouse furin complexed with decanoyl–Arg–Val–Lys–Arg–chloromethylketone (dec–RVKR–cmk) [13] has paved the way for the design of effective inhibitors. Peptidyl chloroalkylketones [14] and an engineered serpin, α_1-antitrypsin Portland (α_1-PDX) [15,16], have been shown to block the furin-dependent processing of envelope glycoproteins of pathogenic viruses, however, the cellular mechanisms controlling the activity of furin are largely unknown.

2. Materials and methods

2.1. Materials

Plasmid pcDNA3.1+, vector pCR4-TOPO and His-tagged TEV protease (10 units/μl) were from Invitrogen. Glutathione Sepharose™ 4B, LMW and HMW size marker kits for SDS–PAGE (#17-0446 and #17-0615, respectively) were obtained from Amersham Biosciences. Recombinant human furin (2 units/μl, corresponding to a 22 nM solution of active site titratable material, see Section 2.6) was from NEB. Protino® Ni 2000 columns were from Macherey Nagel. L-pyroglutamyl–Arg–Thr–Lys–Arg–7-amido-4-methylcoumarin (pERTKR-MCA) and dec–RVKR–cmk [17] were from Bachem Biochemika. The monoclonal antibody MON-148 [18] against human furin was from Alexis Biochemicals. Rabbit antibodies directed against a purified GST-Spn4 fusion variant were obtained from Pineda Antikörper Service, Berlin.

2.2. Plasmid constructions

A plasmid coding for a chimeric protein consisting of an N-terminal His-tag, glutathione S-transferase (GST), a TEV protease cleavage site and Spn4A was constructed as follows: An Spn4A cDNA fragment [6] coding for amino acids 33–424 was amplified by PCR using the primers 5′-GGTTCCGCGTGGATCCATGGCTGACGCCGCCCACCA (sense) and 5′-CCCGGGAATTCTCACAGCTCATCATGCTCGCTGGAG (antisense), thus generating a cDNA flanked by *Nco*I and *Eco*RI sites. After cloning (TOPO cloning kit for sequencing, Invitrogen), an internal Spn4A *Nco*I site was replaced by synonymous substitutions (QuikChange® site-directed mutagenesis kit, Stratagene instruction manual). The modified cDNA was digested with *Nco*I and *Eco*RI and ligated into the *Nco*I/*Eco*RI cleaved vector pKM263 [19], resulting in the expression plasmid pGST-Spn4A-1.

For expression in COS-7 cells, an Spn4A cDNA flanked by *Kpn*I and *Eco*RI sites and coding for amino acids 1–424 was subcloned into pcDNA3.1+ cleaved with *Kpn*I and *Eco*RI. To this end, total RNA from *Drosophila melanogaster* Schneider S2 cells [20] was reverse transcribed and amplified using the primer 5′-CGTTTAGGTACCAGTATGGATTATCGTTTGGTGCCATGTGG and the antisense

* Corresponding author. Fax: +49-521-106-6328.
E-mail address: hr@zellkult.techfak.uni-bielefeld.de (H. Ragg).

Abbreviations: α_1-PDX, α_1-antitrypsin Portland; ER, endoplasmic reticulum; GST, glutathione S-transferase; PBS, phosphate buffered saline; PDI, protein disulfide isomerase; RSL, reactive site loop; SI, stoichiometry of inhibition; TEV, tobacco etch virus

0014-5793/$22.00
doi:10.1016/j.febslet.2004.10.003

primer listed above. Sequencing of the construct indicated identity with the previously published Spn4A coding region [6] with the exception of the S2 cell-specific Gly → Val substitution at position 17 in the hydrophobic core of the signal peptide.

2.3. Expression and purification of Spn4A-1

Plasmid pGST-Spn4A-1 was transformed into *Escherichia coli* BL21. Following incubation at 37 °C to an A_{600} of 0.7–1.0 in LB medium (200 ml), isopropyl ß-D-thiogalactopyranoside (0.1 mM) was added. After 3–4 h at 27 °C, cells were harvested, washed and stored at −20 °C. Cells were resuspended in 3.5 ml cold PBS containing 0.5% Triton X-100, 2.5 mM EDTA, 1 mM PMSF, and 75 μl protease inhibitor cocktail (P8849, Sigma) and disrupted by two French press passages (20 000 psi). Following centrifugation (40 min, 8000 × *g* at 4 °C), the soluble fraction was batch adsorbed to Glutathione Sepharose™ 4B. After washing with PBS, 0.5% Triton X-100, followed by 50 mM HEPES, pH 7.5, the fusion protein was eluted with 50 mM HEPES, pH 8.0, containing 10 mM reduced glutathione and stored at −80 °C.

For cleavage with TEV protease, purified GST-Spn4A-1 (0.5 mg) was incubated for 16 h in 50 mM HEPES, pH 8.0, and 10 mM reduced glutathione with 200 units TEV protease at 4 °C. After the addition of NaCl (final concentration: 300 mM), the liberated serpin moiety was separated from the His-tag containing proteins (residual fusion protein, GST and TEV protease) by chromatography on a Protino® Ni 2000 column, equilibrated in 50 mM HEPES, 0.15% Triton X-100, and 300 mM NaCl. The flow-through containing the purified Spn4A-1 was collected and stored at −80 °C. The purity of the preparations was assessed by staining with Coomassie blue after SDS–PAGE [21]. The concentration of the purified proteins was determined by a standard Bradford assay (Pierce).

2.4. Generation and analysis of inhibitor/enzyme complexes

Purified fusion protein or TEV-liberated Spn4A-1 was incubated with titrated human furin at a molar ratio of 8:1 at 25 °C in 100 mM HEPES, pH 7.5, containing 1 mM Ca^{2+} and 0.5% Triton X-100 (kinetic buffer). The reaction products were resolved by reducing SDS–PAGE (10% gels) and analyzed by Western blotting [21]. Antibodies were used at a dilution of 1:20 000 (anti-Spn4 antiserum) or 1:500 (anti-furin antibody).

2.5. Scissile bond analysis

Purified Spn4A-1 (1.25 μg) was incubated in 50 mM HEPES, pH 7.5, containing 1 mM $CaCl_2$ for 2 h at 25 °C in the absence or presence of furin (0.1 μg). After addition of an equal volume of 0.5% TFA, the samples were desalted with ZipTip® C18 following the manufacturer's instructions (Millipore), applied to the MALDI target chip and mixed with 1 μl matrix solution (10 mg/ml sinapic acid in acetonitrile/water (30:70) containing 0.07% TFA). MALDI-TOF/MS spectra (accelerating voltage: 25 kV) were recorded with a Voyager DE instrument (PE Biosystems, Weiterstadt, Germany) equipped with an LSI nitrogen laser and a 1.2 m linear flight tube.

2.6. Enzymatic assays and kinetic methods

Assays (100 μl) were conducted in 96-well microtiter plates at 30 °C in kinetic buffer using a FLUOstar/POLARstar galaxi spectrometer (bmg labtechnologies). Cleavage of the fluorogenic substrate pERTKR-MCA was initiated with 1 unit of human furin and release of 7-amino-4-methylcoumarin (AMC) was monitored at 460 nm (excitation wavelength: 380 nm). The background resulting from spontaneous substrate hydrolysis was subtracted. By non-linear regression (EnzFitter, Biosoft), a value of 20 ± 2 μM was calculated for the Michaelis constant (K_m), using substrate concentrations between 0.3 and 200 μM.

The concentration of catalytically active furin was determined by titrating with the active site-directed inhibitor dec–RVKR–cmk [22]. The enzyme (3 units) was incubated in kinetic buffer with the chloromethylketone (0–67 nM) for 1 h at 30 °C. After 10-fold dilution and addition of pERTKR-MCA to 200 μM, the rate of substrate hydrolysis was measured and plotted versus the inhibitor concentration. A regression line was fitted to the initially linearly decreasing values of residual enzyme activity. The concentration [E_0] of active furin was extrapolated from the intersection with the *x*-axis. Three units of the titrated enzyme (0.011 pmol per unit) were incubated in the same manner with increasing concentrations of Spn4A-1 (0–15 nM, as determined with the Bradford assay).

Progress curves for furin inhibition at different Spn4A-1 concentrations [*I*] were recorded under pseudo first-order conditions using furin at a concentration of 0.11 nM and the substrate pERTKR-MCA [*S*] at 200 μM. The data were fitted to Eq. (1) for slow tight binding inhibition with a steady state velocity of zero [23,24],

$$P = \frac{v_0}{k'}(1 - e^{-k't}) + b \quad (1)$$

where *P* is the fluorescence; v_0, the initial velocity; *t*, the time; *k*′, the apparent first order rate constant; and *b*, the fluorescence at time $t = 0$. Non-linear regression (EnzFitter) provided *k*′ for each [*I*]. By plotting *k*′ versus [*I*], k_{assoc} was obtained from linear regression according to the following equation [25]:

$$k' = \frac{k_{assoc}}{(1 + [S]/K_m)} \cdot [I] \quad (2)$$

2.7. Transfection of COS-7 cells and immunofluorescence analysis

COS-7 cells were cultivated in DMEM containing 10% FCS. The cells were transfected in 4-well Lab-Tek chamber slides (Nunc) with Lipofectamine™ 2000 (Invitrogen) following the supplier's instructions. After 24 h, cells were rinsed with PBS, fixed with −20 °C cold methanol and treated with blocking/washing solution (3% (w/v) BSA in PBS). For immunostaining, the anti-Spn4 rabbit antiserum (Section 2.1) and a FITC labeled anti-rabbit antibody (Sigma, F1262) were used. The ER marker, protein disulfide isomerase (PDI), was localized using a monoclonal mouse antibody (Stressgen, SPA-891) and a Cy3-labeled anti-mouse antibody (Jackson ImmunoResearch Labs, 715-165-150). All antibodies were diluted 100-fold in blocking/washing solution. The cells were mounted with Mowiol 4.88 medium (Calbiochem). Fluorescence was examined with an Olympus IX81 epifluorescence microscope (40× objective) equipped with a Hamamatsu C8484-05G camera. Color and intensity adjustments of the pictures and the overlay were performed with Adobe Photoshop, version 7.

3. Results

3.1. Recombinant expression

To produce Spn4A-1 in sufficient amounts and purity, we constructed an expression plasmid coding for a fusion protein consisting of isoform Spn4A connected via a TEV protease cleavage site sequence to the N-terminal GST (containing a His-tag at its N-terminal end). The chimera was isolated from the bacterial cytosol and purified on Glutathione Sepharose™ 4B. After cleavage with TEV protease, all His-tagged components (residual fusion protein, cleaved GST and TEV protease) were removed by metal affinity chromatography. Analysis by SDS–PAGE (Fig. 1) showed that highly purified Spn4A-1 had been obtained, which was expected to include two additional amino acids (Gly-Ala) at its N-terminus as a result of TEV protease cleavage.

3.2. Complex formation with furin

Incubation of Spn4A-1 – either in the fused or in TEV protease liberated form – with human furin resulted in the formation of SDS stable complexes (Fig. 2) as demonstrated by Western blotting, using antibodies directed against the fusion protein or against human furin, respectively. The apparent sizes of the complexes were ~135 and ~115 kDa, respectively, depending on whether the fused serpin or TEV cleaved Spn4A-1 was used. Enzyme/inhibitor complexes were detected after only 20 s of incubation (not shown). A fraction of the serpin migrated at an increased rate (39 kDa) after incubation with furin, in accordance with the branched pathway mechanism of serpins [3]. The ~53 kDa band corresponding to free furin did not appear when denaturation was performed at

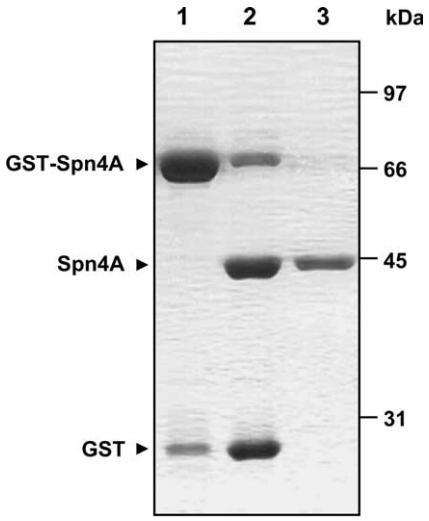

Fig. 1. Isolation of Spn4A-1. GST-Spn4A-1 was purified from bacterial extracts via Glutathione Sepharose™ 4B (lane 1) and treated with TEV protease (lane 2). His-tagged components were removed by metal affinity chromatography (lane 3). Proteins were stained with Coomassie brilliant blue after SDS–PAGE (10% gels). The positions of the size markers are given on the right.

low stringency (5 min at 56 °C, not shown), indicating that the complex dissociates only under harsh conditions.

3.3. Identification of the scissile bond

Spn4A contains the sequence RRKRA within its RSL (positions 371–375) that closely resembles the furin recognition/cleavage site RXR/KR↓. In order to identify the actual P1–P1′ positions of Spn4A-1, the inhibitor was co-incubated with furin followed by MALDI-TOF/MS analysis of the reaction products. Cleavage of Spn4A-1 (calculated average mass: 44255.6 Da) at the furin consensus sequence was expected to generate fragments of 38454.1 and 5819.5 Da, respectively. Fig. 3 shows that furin cleavage of Spn4A-1 resulted in the appearance of a fragment at $m/z = 38422.5$ and a set of fragments at $m/z = 5000$–6000 that included a fragment at $m/z = 5819.5$ as most intense signal, in accordance with the furin cleavage site. No such signals were observed with untreated Spn4A-1 (control), indicating that these signals were not due to unspecific proteolysis. The data thus show that Arg–Ala constitute positions P1–P1′ for the interaction with furin. Moreover, alternative basic amino acids are not used as P1 residues (expected average masses: 5975.7; 6103.9; and 6260.1 Da).

3.4. Inhibition of furin

For determining the stoichiometry of inhibition (SI), furin was titrated with the active site directed inhibitor dec–RVKR–cmk and Spn4A-1, respectively. We calculated an SI value of about 3.5 and a 4.5-fold excess of the serpin was found to be sufficient to abolish furin activity completely. To determine the apparent association rate constant, the enzyme was incubated with increasing amounts of purified Spn4A-1 using an at least 10-fold excess of inhibitor to meet pseudo-first order conditions and progress curves reflecting the interaction between furin and the serpin were recorded (Fig. 4). The fluorescence reached a limit value and there was no return of enzyme activity for at least 24 h of incubation (not shown). Using non-linear regression analysis, an apparent k_{assoc} of $(5.5 \pm 0.5) \times 10^6$ M^{-1} s^{-1} was calculated.

3.5. Subcellular localization of Spn4A in transfected COS-7 cells

To investigate the potential role of Spn4A as a cellular regulator of furin-like enzymes in the ER and secretory routes, COS-7 cells were transfected with a plasmid coding for Spn4A containing the genuine signal peptide and the C-terminal

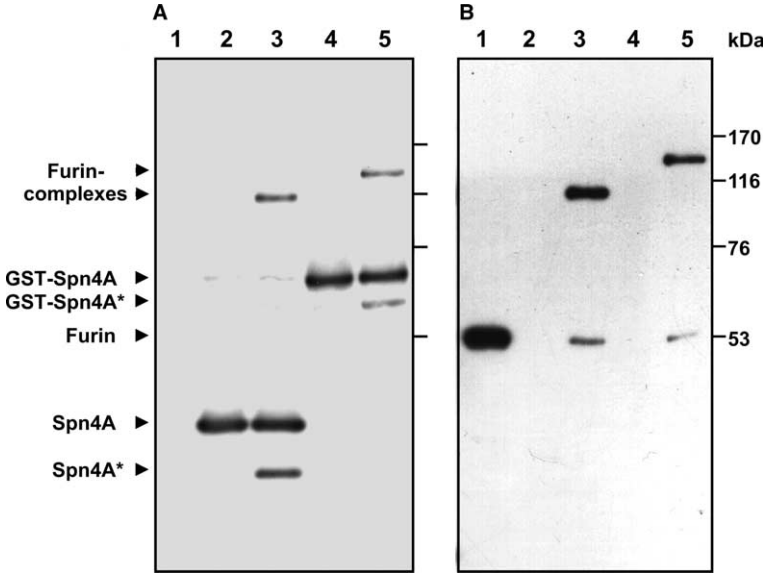

Fig. 2. Complex formation between Spn4A-1 and furin. Fused or TEV-cleaved Spn4A-1 was incubated for 2 min with furin in the presence of Ca^{2+} and boiled for 4 min in reducing SDS-PAGE buffer. After electrophoresis (10% gels), the reaction products were analyzed by Western blotting, using antibodies directed against GST-Spn4 (A) or human furin (B). Lane 1, furin; lane 2, Spn4A-1; lane 3, Spn4A-1 incubated with furin; lane 4, GST-Spn4A-1; and lane 5, GST-Spn4A-1 incubated with furin. The furin-cleaved forms of GST-Spn4A-1 and Spn4A-1 are marked by an asterisk. The positions of the size markers are given on the right side of each panel.

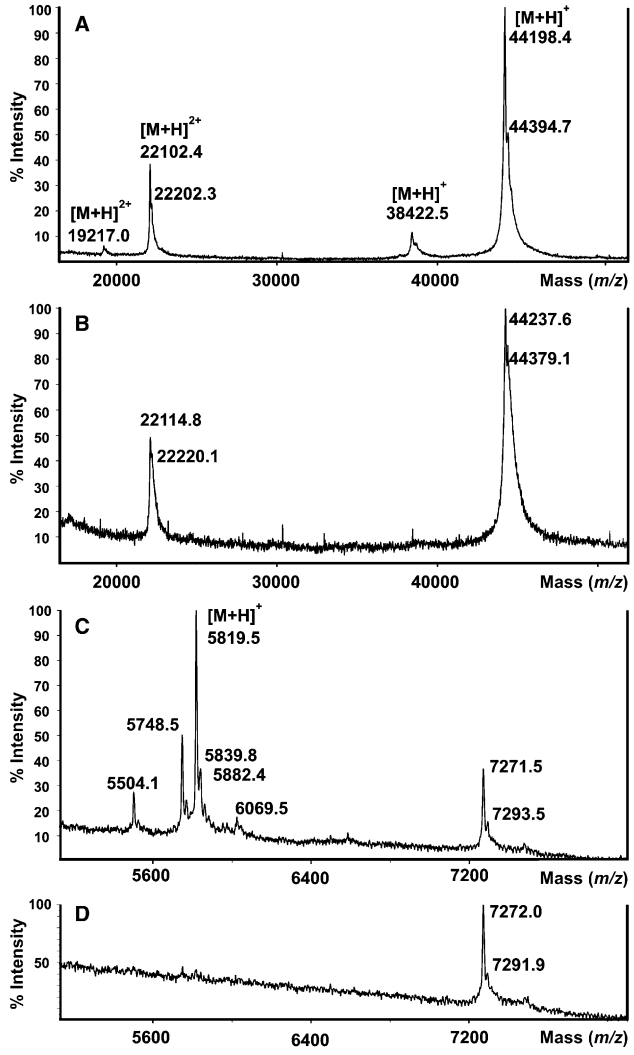

Fig. 3. Identification of the scissile bond. Purified Spn4A-1 (calculated average mass: 44255.6 Da) was incubated with human furin followed by MALDI-TOF/MS. Consistent with the expected cleavage site, signals at $m/z = 38422.5$ (A) and 5819.5 (C) are observed that are not present in the untreated control (B, D).

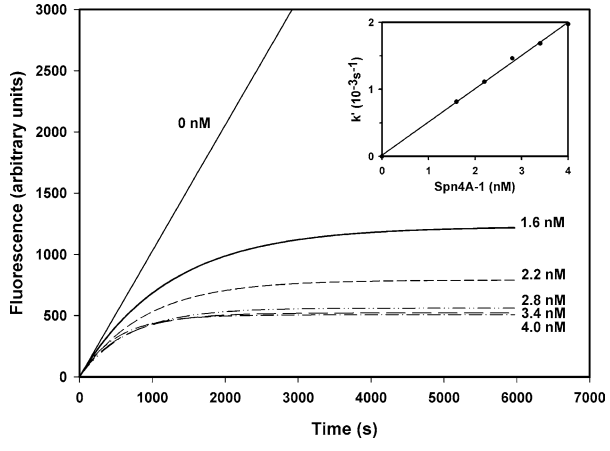

Fig. 4. Progress curves for the inhibition of human furin (0.11 nM) by Spn4A-1 (0–4.0 nM). The inset shows that k' linearly depends on the Spn4A-1 concentration. The apparent constant k_{assoc} was derived from the slope of the regression line (Section 2.6).

HDEL sequence or with pcDNA3.1+, and a double immunostaining analysis was performed. The established ER marker PDI [26] was detected in all cells with a characteristic perinuclear staining pattern (Fig. 5A). In contrast, only cells transfected with the Spn4A expression plasmid (Fig. 5B) showed a marked FITC fluorescence that did neither occur in cells transfected with the empty vector nor using the secondary antibody alone or in combination with a rabbit control serum (not shown). The FITC fluorescence showed the same subcellular distribution as that of Cy3, demonstrating co-localization of Spn4A and PDI (Fig. 5C). The experiment thus indicates that the genuine N-terminal signal peptide and the HDEL sequence of Spn4A mediate import and retention of the fruit fly serpin in the ER of mammalian cells.

4. Discussion

The present communication demonstrates that a recombinant serpin Spn4A variant, that differs solely by an N-terminal extension of two amino acids from the genuine sequence, forms SDS-stable complexes with human furin. The inhibitor is cleaved C-terminally to the sequence RRKR, in agreement with the recognition/cleavage site of the prohormone convertase. The co-localization of Spn4A with the ER marker PDI in transfected COS-7 cells and the kinetic parameters of Spn4A/furin interaction suggest that Spn4A may be a physiological regulator of furin and/or related targets. The bacterially expressed serpin inhibits furin with a high apparent k_{assoc} of 5.5×10^6 M^{-1} s^{-1}. Correcting for the SI of the reaction [3], an overall k_{assoc} of 1.9×10^7 M^{-1} s^{-1} was extrapolated from these data, a value that is comparable to that determined by Richer et al. [27] for N-terminally His-FLAG-tagged Spn4A ($k_{assoc} = 3.2 \times 10^7$ M^{-1} s^{-1}, SI $\sim$ 1). Using C-terminally His-tagged Spn4A extracted from sonicated bacteria, Osterwalder et al. [28] calculated an apparent k_{assoc} of 2.1×10^5 M^{-1} s^{-1} for inhibition of human furin (determined at 22 °C) and an eightfold molar excess of the inhibitor was necessary to achieve 65% reduction of the enzyme's amidolytic activity. These apparent differences could be due to several different factors, including (i) effects exerted by the varying positions and sequences of the tags used for the expression constructs, (ii) the conditions employed for preparation and storage of the recombinant serpin, (iii) the different enzyme/inhibitor ratios used for determining the kinetic parameters and (iv) the strongly temperature-dependent partition of Spn4A between the inhibitory and the substrate pathway of serpins [27].

A few other serpins have been shown to inhibit furin. The genetically engineered serpin α_1-PDX, which contains the sequence RIPR within its RSL [15], inhibits furin with a k_{assoc} of 1.5×10^6 M^{-1} s^{-1} [29] and for human protease inhibitor 8 (PI8), a k_{assoc} value of 6.5×10^5 M^{-1} s^{-1} was determined [30]. In order to control furin at its cellular locations, inhibitors must gain access to the secretory pathway. PI8 does not contain the cleavable N-terminal signal peptide required for entering the ER and histochemical investigations localize human PI8 primarily within the nucleus [31] in contrast to the genetically engineered α_1-PDX that is predominantly found within the *trans*-Golgi network [32]. The subcellular distribution of Spn4A in transfected COS-7 cells suggests that the inhibitor may represent the first natural serpin that can be retrieved to

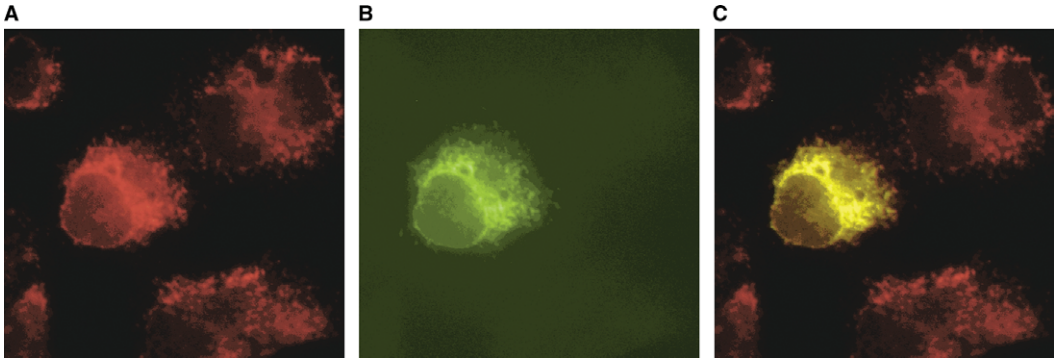

Fig. 5. Intracellular localization of Spn4A. COS-7 cells were transfected with an expression plasmid coding for Spn4A, including the genuine signal peptide and the C-terminal HDEL sequence. Cells were fixed and prepared for immunostaining as described in Section 2.7. (A) Cy3 immunofluorescence of the ER marker PDI; (B) FITC fluorescence of cells expressing Spn4A; (C) overlay of FITC- and Cy3 fluorescence demonstrating co-localization of SpnA and PDI.

the ER and therefore can inhibit furin-like enzymes within the secretory routes of eukaryotic cells. In *Drosophila melanogaster*, two genes coding for furin homologs have been identified [33–35], which could be possible targets for Spn4A. Genetic [28] and biochemical experiments [27] indicate that Spn4A may control Amontillado, the *Drosophila* homolog of the mammalian prohormone convertase PC2 [36,37]. Further targets could include subtilase-like enzymes from pathogens that invade cells via the secretory pathway.

Acknowledgements: We gratefully acknowledge the contributions of S. Brinkmeyer and M. Lummer in this project. This work was supported in part by Deutsche Forschungsgemeinschaft, Graduiertenkolleg 'Zelluläre Grundlagen biotechnischer Prozesse'.

References

[1] LeMosy, E.K., Hong, C.C. and Hashimoto, C. (1999) Trends Cell. Biol. 9, 102–107.
[2] Krem, M.M. and Di Cera, E. (2002) Trends Biochem. Sci. 27, 67–74.
[3] Gettins, P.G.W. (2002) Chem. Rev. 102, 4751–4804.
[4] Rubin, G.M., Yandell, M.D., Wortman, J.R., Gabor Miklos, G.L., Nelson, C.R., Hariharan, I.K., Fortini, M.E., Li, P.W., Apweiler, R. and Fleischmann, W., et al. (2000) Science 287, 2204–2215.
[5] Han, J., Zhang, H., Min, G., Kemler, D. and Hashimoto, C. (2000) FEBS Lett. 468, 194–198.
[6] Krüger, O., Ladewig, J., Köster, K. and Ragg, H. (2002) Gene 293, 97–105.
[7] Nakayama, K. (1997) Biochem. J. 327, 625–635.
[8] Steiner, D.F. (1998) Curr. Opin. Chem. Biol. 2, 31–39.
[9] Rockwell, N.C., Krysan, D.J., Komiyama, T. and Fuller, R.S. (2002) Chem. Rev. 102, 4525–4548.
[10] Thomas, G. (2002) Nat. Rev. Mol. Cell Biol. 3, 753–766.
[11] Teuchert, M., Berghofer, S., Klenk, H.D. and Garten, W. (1999) J. Biol. Chem. 274, 36781–36789.
[12] Anderson, E.D., Molloy, S.S., Jean, F., Fei, H., Shimamura, S. and Thomas, G. (2002) J. Biol. Chem. 277, 12879–12890.
[13] Henrich, S., Cameron, A., Bourenkov, G.P., Kiefersauer, R., Huber, R., Lindberg, I., Bode, W. and Than, M.E. (2003) Nat. Struct. Biol. 10, 520–526.
[14] Garten, W., Hallenberger, S., Ortmann, D., Schafer, W., Vey, M., Angliker, H., Shaw, E. and Klenk, H.D. (1994) Biochimie 76, 217–225.
[15] Anderson, E.D., Thomas, L., Hayflick, J.S. and Thomas, G. (1993) J. Biol. Chem. 268, 24887–24891.
[16] Jean, F., Thomas, L., Molloy, S.S., Liu, G., Jarvis, M.A., Nelson, J.A. and Thomas, G. (2000) Proc. Natl. Acad. Sci. USA 97, 2864–2869.
[17] Angliker, H., Wikstrom, P., Shaw, E., Brenner, C. and Fuller, R.S. (1993) Biochem. J. 293, 75–81.
[18] van Duijnhoven, H.L., Creemers, J.W., Kranenborg, M.G., Timmer, E.D., Groeneveld, A., van den Ouweland, A.M., Roebroek, A.J. and van de Ven, W.J. (1992) Hybridoma 11, 71–86.
[19] Melcher, K. (2000) Anal. Biochem. 277, 109–120.
[20] Schneider, I. (1972) J. Embryol. Exp. Morph. 27, 353–365.
[21] Böhme, C., Nimtz, M., Grabenhorst, E., Conradt, H.S., Strathmann, A. and Ragg, H. (2002) Eur. J. Biochem. 269, 977–988.
[22] Jean, F., Stella, K., Thomas, L., Liu, G., Xiang, Y., Reason, A.J. and Thomas, G. (1998) Proc. Natl. Acad. Sci. USA 95, 7293–7298.
[23] Morrison, J.F. and Walsh, C.T. (1988) Adv. Enzymol. Relat. Areas Mol. Biol. 61, 201–301.
[24] Dufour, E.K., Denault, J.B., Bissonnette, L., Hopkins, P.C., Lavigne, P. and Leduc, R. (2001) J. Biol. Chem. 276, 38971–38979.
[25] Bieth, J.G. (1995) Methods Enzymol. 248, 59–84.
[26] Schweizer, A., Rohrer, J., Slot, J.W., Geuze, H.J. and Kornfeld, S. (1995) J. Cell Sci. 108, 2477–2485.
[27] Richer, M.J., Keays, C.A., Waterhouse, J., Minhas, J., Hashimoto, C. and Jean, F. (2004) Proc. Natl. Acad. Sci. USA 101, 10560–10565.
[28] Osterwalder, T., Kuhnen, A., Leiserson, W.M., Kim, Y.S. and Keshishian, H. (2004) J. Neurosci. 24, 5482–5491.
[29] Dufour, E.K., Denault, J.B., Hopkins, P.C. and Leduc, R. (1998) FEBS Lett. 426, 41–46.
[30] Dahlen, J.R., Jean, F., Thomas, G., Foster, D.C. and Kisiel, W. (1998) J. Biol. Chem. 273, 1851–1854.
[31] Strik, M.C., Bladergroen, B.A., Wouters, D., Kisiel, W., Hooijberg, J.H., Verlaan, A.R., Hordijk, P.L., Schneider, P., Hack, C.E. and Kummer, J.A. (2002) J. Histochem. Cytochem. 50, 1443–1454.
[32] Benjannet, S., Savaria, D., Laslop, A., Munzer, J.S., Chretien, M., Marcinkiewicz, M. and Seidah, N.G. (1997) J. Biol. Chem. 272, 26210–26218.
[33] Roebroek, A.J., Pauli, I.G., Zhang, Y. and van de Ven, W.J. (1991) FEBS Lett. 289, 133–137.
[34] Hayflick, J.S., Wolfgang, W.J., Forte, M.A. and Thomas, G. (1992) J. Neurosci. 12, 705–717.
[35] Roebroek, A.J., Ayoubi, T.A., Creemers, J.W., Pauli, I.G. and van de Ven, W.J. (1995) DNA Cell Biol. 14, 223–234.
[36] Siekhaus, D.E. and Fuller, R.S. (1999) J. Neurosci. 19, 6942–6954.
[37] Hwang, J.R., Siekhaus, D.E., Fuller, R.S., Taghert, P.H. and Lindberg, I. (2000) J. Biol. Chem. 275, 17886–17893.